# A Frequency-Based Determination of Transient Inductance and Rotor Resistance for Field Commissioning Purposes

Russel J. Kerkman, *Senior Member, IEEE,* Jerry D. Thunes, *Member, IEEE,*
Timothy M. Rowan, *Member, IEEE,* and David W. Schlegel, *Student Member, IEEE*

***Abstract*— The paper presents a deterministic method of estimating the transient inductance and rotor resistance of an induction machine for field commissioning purposes. The parameter values obtained by the method are compared with those for a transient method of commissioning. Skin effects inherent with the transient test are documented. Experimental results for a wide range of machine sizes are included for both methods. The quality of field orientation is established for each method through experimental testing.**

## I. Introduction

FIELD orientation (FO) is the preferred control strategy for medium- and high-performance applications. Field-oriented controllers (FOC) may be classified as direct (DFOC), indirect (IFOC), stator or flux vector (FV), and direct self-control (DSC). Each approach provides excellent steady-state characteristics, but their transient behaviors differ. Ultimately the performance of the controllers depends on the accuracy of the respective motor parameters employed by the control algorithm. For example, an IFOC employing an inaccurate estimate of the induction motor's rotor time constant may compromise performance to the extent the drive fails to meet the application requirements.

To maintain the expected performance of a FO drive, parameter adaptation methods were developed. The technical literature reflects two broad categories of parameter adaptation. One employs extended Kalman filtering techniques to estimate unmeasureable states and update machine parameters [1]. The other technique incorporates a model reference adaptive control (MRAC) to adjust the control parameters to reflect motor parameter changes [2]. Regardless of the approach, the control parameters require initialization. Therefore, an accurate self or field commissioning procedure is a prerequisite to obtaining the high performance expected of FOC.

Field commissioning of ac drives has recently received considerable attention [3], [4]. The commissioning procedures appearing in the technical literature follow two main categories: statistical and deterministic. Statistical procedures employ estimation theory to establish initial parameters minimizing an error function, often in a least squares sense [5]. Deterministic techniques conduct tests to extract the needed control parameters [6]. Deterministic techniques are further divided into transient and steady-state excitation approaches [4], [6], [7].

The paper begins by examining the transient method of determining the induction machine's transient inductance. This method is evaluated by experimental and performance testing of the motor drive system. The corrupting influence of skin effect is demonstrated and its effect on drive performance presented. The frequency-based commissioning procedure is then presented. Through steady-state analyses and simulations, a procedure for single-phase excitation is established. The procedure maintains a locked rotor condition and reduces the adverse effects of skin effect on the measurement of the transient inductance and rotor resistance. Results from tests performed on machines from 7.5 to 1250 hp are included. The commissioning values are evaluated by examining the torque linearity and FO.

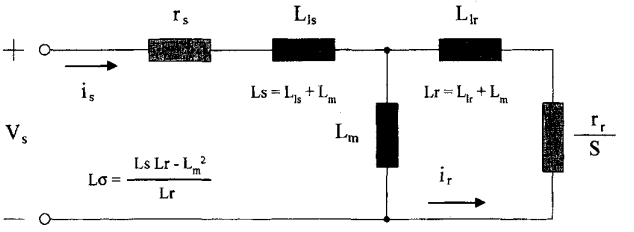


Fig. 1. Single-phase motor model.

## II. The Transient Method of Determining the Transient Inductance

### A. Analysis

Transient testing of the induction machine was one of the first self-commissioning techniques [3], [8]. The single-phase equivalent circuit of the induction motor is shown in Fig. 1. The transient test consists of single-phase pulsing the induction motor and measuring the elapsed time between preset values of current. The impedance obtained represents the transient inductance of Fig. 1.

Paper 95–85, approved by the Industrial Drives Committee of the IEEE Industry Applications Society for presentation at the 1995 IEEE Industry Applications Society Annual Meeting, Lake Buena Vista, FL, October 8–12. Manuscript released for publication December 8, 1995.

The authors are with Allen-Bradley Company, Standard Drives Business, Mequon, WI 53092 USA.

Publisher Item Identifier S 0093-9994(96)02966-0.

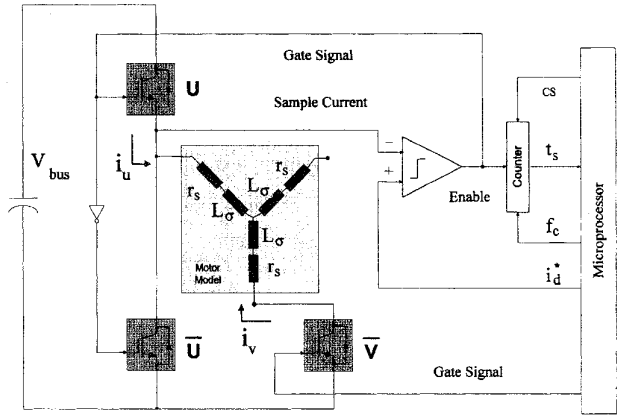


Fig. 2. Transient test structure.

A typical test structure is shown in Fig. 2. The counter is enabled simultaneously with the turn-on of two power devices; it continues to count until the phase current equals the desired current $i_d^*$. When the current equals the commanded current, the motor leads are shorted and the time $t_{s1}$ latched. The equation for the transient inductance becomes

$$L_\sigma = (I_{\rm ss} r_s t_{s1})/i_d^*. \tag{1}$$

Here, $r_s$ is the measured stator resistance, $I_{\rm ss}$ is the steady-state $d$-axis current, and $i_d^*$ the desired current value (e.g., $i_{\rm rated}$) is given by (2). The steady-state current is given by (3)

$$i_d^* = (i_u - i_v)/\sqrt{3} \tag{2}$$

$$I_{\rm ss} = I_d = V_{\rm bus}/(\sqrt{3} r_s). \tag{3}$$

This estimate of the transient inductance follows from the Taylor series expansion for the exponential of the reduced order equation of the $d$-axis current, (4) and (5)

$$i(t) = I_d(t) = I_{\rm ss}\left(1 - e^{\frac{-r_s}{L_\sigma} t}\right) \tag{4}$$

$$i(t) = I_{\rm ss}\left(1 - 1 + \frac{r_s}{L_\sigma} t\right) = I_{\rm ss}\frac{r_s}{L_\sigma} t. \tag{5}$$

As pointed out by Schierling, the assumptions and associated limitations of this approach to establishing the transient inductance can limit the accuracy of the results. For example, skin and eddy current effects can produce too small a result; thus, alternatives to the simple test were developed. One alternate approach repeats the previous test, but after shorting the terminals waits a sufficient time and reverses the applied voltage. Reversing the voltage drives the current in the opposite direction. With this test it is best to calculate $L_\sigma$ from the numerical derivative. The technique is explained through (6)

$$L_\sigma = (V_{\rm bus} t_{s2})/(i_{s1} - i_{s2})/\sqrt{3}. \tag{6}$$

Here, $i_{s1}$ is the current before reversing the bus voltage, and $i_{s2}$ is the current at $t_{s2}$ after voltage reversal.

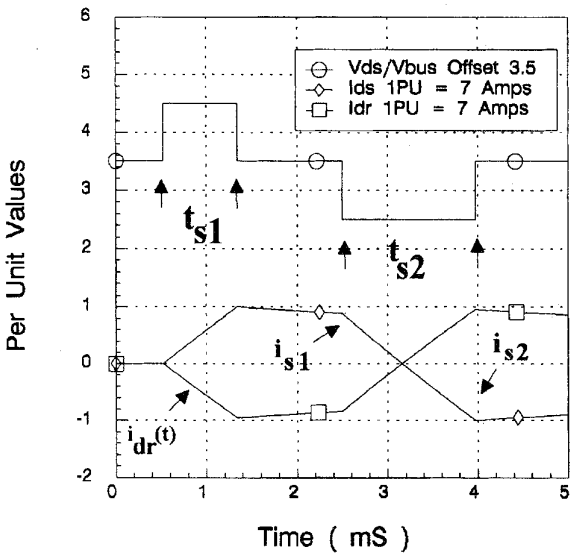


Fig. 3. Simulation of transient test for determining $L_\sigma$.

Fig. 3 shows simulation results for both approaches applied to the $d$-axis topology. The first method calculates a transient inductance of 29.41 mH; the second method 28.33 mH. The actual value is 28.10 mH, based on the 5-hp machine parameters listed in the appendix. The alternative approach significantly increases the accuracy of the transient test.

### *B. Experimental Evaluation of the Transient Technique*

Tests were performed on induction motors encompassing a wide range of horsepowers. Transient inductance values were obtained from dynamometer testing and correspond to field-oriented conditions and are referred to as tuned values. The tuned values were compared to values obtained from the transient technique. For example, results for a 20-hp, 4-pole, 460-V induction motor are displayed in Fig. 4. The tuned value for the transient inductance is 6.79 mH [2]. The transient test, however, resulted in a value of 4.30 mH, an error of 38%.

A Monte Carlo simulation was performed to assess the error in torque due to incorrect MRAC values for the transient inductance. The results for a $+/-10\%$ error in the transient inductance are shown in Fig. 5. The motors investigated ranged from 5 to 300 hp. The torque command increment was 0.25 p.u. The analysis shows the largest error, $-10\%$, occurs at $-10\%$ error in the estimated transient inductance for a 100-hp machine with 1 p.u. torque command.

An experimental investigation of the above findings was performed. Results for a 5-hp machine are shown in Fig. 6. The worst case for a $\pm 10\%$ error in the MRAC's reference value of the transient inductance occurs at 1 p.u. and results in $\pm 4\%$ error in torque. This agrees favorably with the results of Fig. 5.

As suggested above, skin effects corrupt high frequency measurements of the transient inductance. This becomes more of a problem with increasing horsepower due to the construction of the rotor. To establish the extent skin effect has on the results of Fig. 4, the rotor was removed and the test repeated.

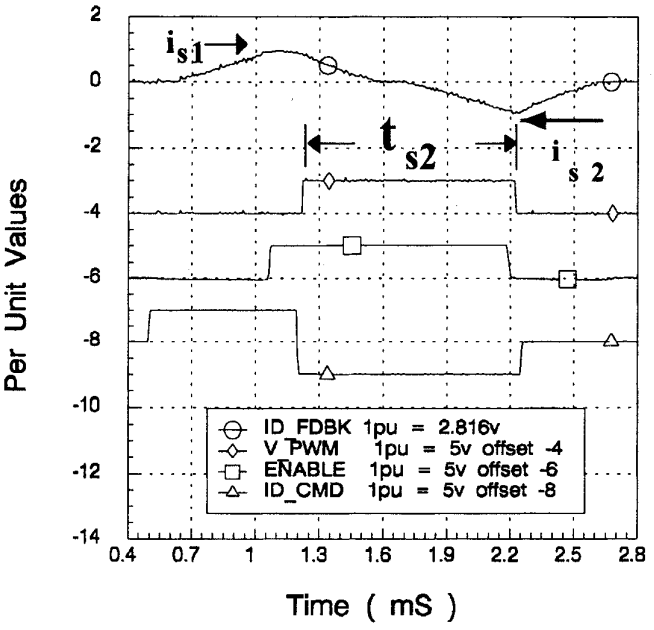


Fig. 4. Experimental results of transient test for determining $L_\sigma$.

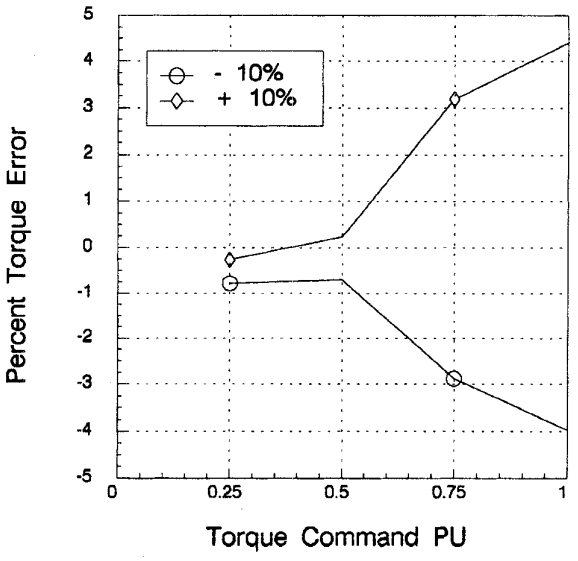


Fig. 6. Experimental results showing torque error for $\pm 10\%$ $L_\sigma$ error in MRAC [2].

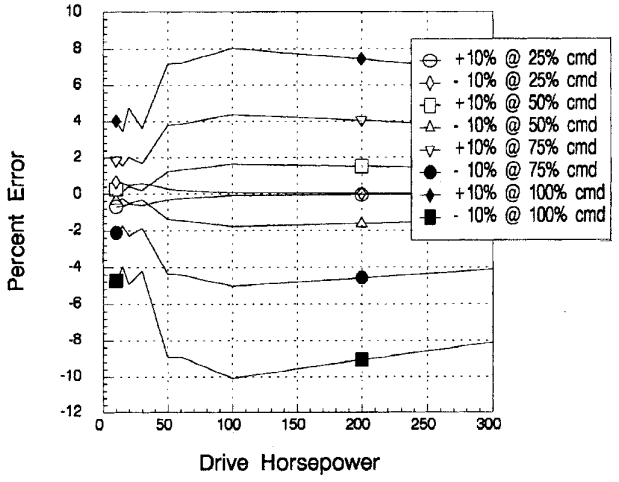


Fig. 5. Torque error for $\pm 10\%$ $L_\sigma$ error with MRAC [2]—Monte Carlo simulation.

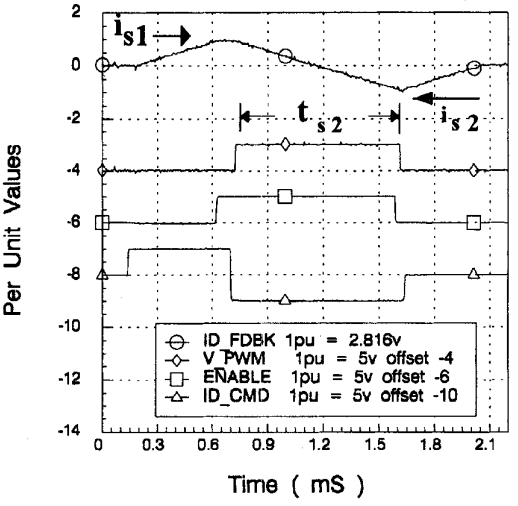


Fig. 7. Experimental results for transient test with rotor removed.

The results are shown in Fig. 7. A transient inductance of 3.82 mH was calculated from the measurements, which is close to the value with the rotor installed. Additional tests confirm the presence of the rotor to have a minimal effect on the transient inductance obtained with this technique. Therefore, the transient test yields an estimate of the machine's transient inductance that is consistently lower than the tuned value.

## III. A Frequency-Based Transient Inductance Identifier

### A. Single-Phase Model

Other approaches to establishing the control parameters for FO and DSC have appeared in the technical literature [6], [7], [9]. Often the intent is to determine the rotor time constant or operating point dependent parameters; for example, the magnetizing inductance. In this section of the paper, single phase sinusoidal excitation of the machine will be analyzed for purposes of establishing the transient inductance and initial rotor resistance for a MRAC.

Fig. 1 shows the single-phase model of the induction machine. Setting the slip to unity corresponds to single-phase operation of the machine with the rotor at stand still. The input impedance for this circuit is given by (7). Both the effective resistance and inductance are functions of $\omega_e$, the electrical frequency

$$Z_{\text{th}} = r_s + r_r \frac{\omega_e^2 L_m^2}{r_r^2 + \omega_e^2 (L_{lr} + L_m)^2} + j\omega_e \left( L_{ls} + \frac{L_m \left[ \omega_e^2 L_{lr} \{ L_{lr} + L_m \} + r_r^2 \right]}{r_r^2 + \omega_e^2 (L_{lr} + L_m)^2} \right). \quad (7)$$

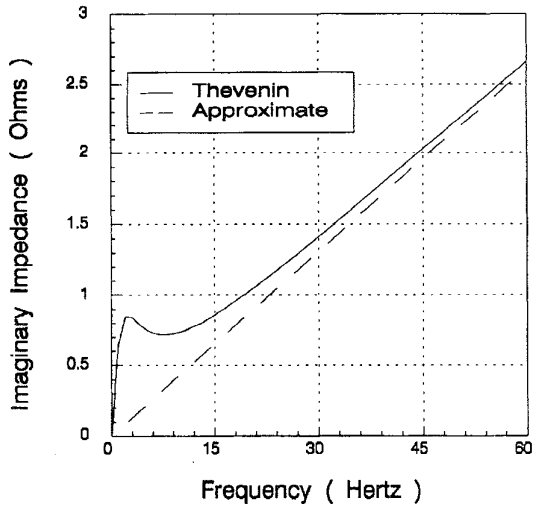


Fig. 8. Frequency analysis of imaginary part of motor impedance.

The imaginary part of the impedance is plotted in Fig. 8 for a 10-hp induction motor. The parameters are included in the Appendix. In addition, the imaginary part of the impedance corresponding to the approximate model given by (8) is also included. This approximate model is simply the series combination of the stator and rotor resistances and the transient inductance. As the operating frequency increases, the two models converge to the same values; the imaginary part approaching the transient inductance and the real part the sum of the stator and rotor resistances. This analysis suggests the transient inductance and rotor resistance of an induction machine can be obtained by single phase sinusoidal excitation

$$Z_{\text{app}} = r_s + r_r + j\omega_e\left(\frac{(L_{ls}+L_m)(L_{lr}+L_m) - L_m^2}{(L_{lr}+L_m)}\right) = r_s + r_r + j\omega_e L_\sigma. \tag{8}$$

### B. The Synchronous Frame Model

Single-phase excitation of an induction motor may also be analyzed from the viewpoint of multiple reference frames [10]; in this case, the applied voltage or current is resolved into forward and reverse components. For single-phase excitation at locked rotor with a current-regulated pulse-width modulated (PWM) inverter, the system equations for the forward components become

$$\begin{bmatrix} V_q \\ V_d \\ 0 \\ 0 \end{bmatrix} = \begin{bmatrix} r_s & \omega_e L_s & 0 & \omega_e L_m \\ -\omega_e L_s & r_s & -\omega_e L_m & 0 \\ 0 & \omega_e L_m & r_r & \omega_e L_r \\ -\omega_e L_m & 0 & -\omega_e L_r & r_r \end{bmatrix} \begin{bmatrix} 0 \\ \frac{I_d}{2} \\ i_{qr} \\ i_{dr} \end{bmatrix}. \tag{9}$$

With the stator currents regulated, the rotor currents are easily solved for in terms of the inputs resulting in (10a). For sufficiently large $\omega_e$, the rotor currents are given by (10b). Substituting (10b) into the stator voltage equations of (9) and assuming unity for the ratio of magnetizing to rotor inductance yields (11), which may be solved for the transient inductance

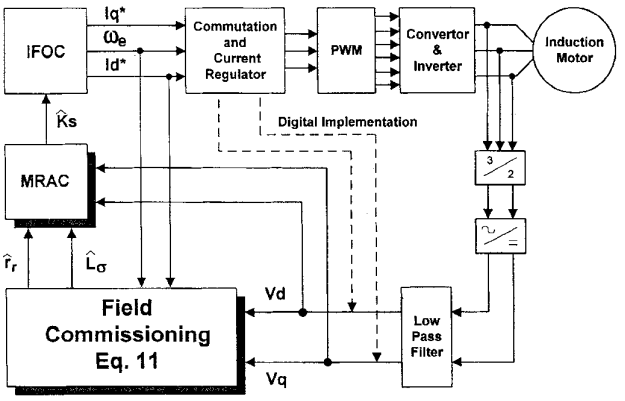


Fig. 9. System block diagram.

and series combination of stator and rotor resistances

$$\begin{bmatrix} i_{qr} \\ i_{dr} \end{bmatrix} = \begin{bmatrix} \frac{-\omega_e L_m r_r}{r_r^2+\omega_e^2 L_r^2} \\ \frac{-\omega_e^2 L_m L_r}{r_r^2+\omega_e^2 L_r^2} \end{bmatrix} \frac{I_d}{2} \tag{10a}$$

$$\begin{bmatrix} i_{qr} \\ i_{dr} \end{bmatrix} \cong \begin{bmatrix} \frac{-L_m r_r}{\omega_e L_r^2} \\ \frac{-L_m}{L_r} \end{bmatrix} \frac{I_d}{2} \tag{10b}$$

$$\begin{bmatrix} V_q \\ V_d \end{bmatrix} = \begin{bmatrix} \omega_e \frac{(L_s L_r - L_m^2)}{L_r} \\ r_s + r_r \end{bmatrix} \frac{I_d}{2} = \begin{bmatrix} \omega_e L_\sigma \\ r_s + r_r \end{bmatrix} \frac{I_d}{2}. \tag{11}$$

Equation (11) shows the transient inductance and rotor resistance are easily obtained. First, excite the motor with single-phase current and measure the synchronous voltages $(V_q, V_d)$. The transient inductance $(L_\sigma)$ equals the $q$-axis voltage divided by the product of the operating frequency and one-half of the excitation current $(\omega_e I_d/2)$. The sum of the rotor and stator resistances equals the $d$-axis voltage divided by one-half of the excitation current. The rotor resistance is then determined by subtracting the stator resistance, obtained from a separate dc test, from the sum.

### C. Simulation Results and System Configuration

The operating frequency and current level are critical factors in obtaining accurate tuning parameters for IFOC. The operating frequency must be sufficiently large to guarantee the validity of the approximation, but not too large as to corrupt the measurement with skin effects. In addition, the current level will affect the results due to the saturation of the leakage paths.

Steady-state analyses were performed on machines from 2 to 1250 hp using manufacturers' design data to establish an estimate of the excitation frequency. The study showed an operating frequency of 30 Hz provided convergence to within 2% of the machine's transient inductance and a value of rotor resistance to within 12% of the design values.

Computer simulations investigated the implementation, signal quality, and filtering requirements prior to implementation. Fig. 9 shows a block diagram of the system. The field commissioning module's inputs include the terminal voltages (either measured or inferred), the excitation frequency, and current level. The signal-level synchronous voltages are low-pass filtered and along with the excitation current serve as inputs in (11). The outputs from the commissioning module—the transient inductance and rotor resistance—serve as inputs to the

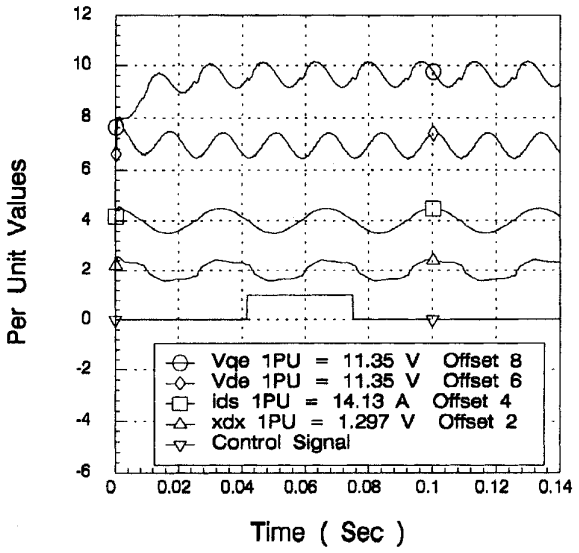


Fig. 10. Simulation results for single-phase excitation.

MRAC [2]. The MRAC together with the IFOC dynamically control the induction motor to maintain FO throughout the operating region.

Fig. 10 shows simulation results for single-phase excitation of a 5-hp induction motor with a carrier frequency of 2 kHz. The top two traces show the $q$ and $d$ feedback voltages in the synchronous frame, followed by the $d$-axis current feedback, the $d$-axis current regulator's integral in the stator frame, and a control signal indicating the period of data collection.

Applying the synchronous frame technique with an excitation frequency of 30 Hz, the algorithm estimated the machine's transient inductance at 28.60 mH. This compares favorably with the calculated value of 28.10 mH. The estimated rotor resistance was 0.8161 Ω as compared to 0.8556 Ω used in the motor model. Both values are within the limits established by the steady-state analyses.

## IV. Experimental Results

The single-phase excitation method was implemented with a current-regulated pulse-width modulated (CRPWM) inverter drive system as outlined in Fig. 9. The entire self-commissioning and MRAC algorithms were executed within a single Intel 80196 microcontroller. Typical waveforms are displayed in Fig. 11. Fig. 11(a) shows the current command, current feedback, and synchronous $d$-$q$ axes feedback voltages. Fig. 11(b) shows the same quantities, but with the voltages ac coupled to amplify the twice-fundamental components.

The synchronous frame is convenient for processing the sampled data and establishing the self-commissioned values of the transient inductance and rotor resistance. The synchronous feedback voltages have an inherent double frequency component from the negative sequence present when excited by single-phase current control. By passing the voltage values through digital filters and taking advantage of the known harmonic content, simple averaging techniques may be applied to greatly reduce the "noise" and double-frequency components

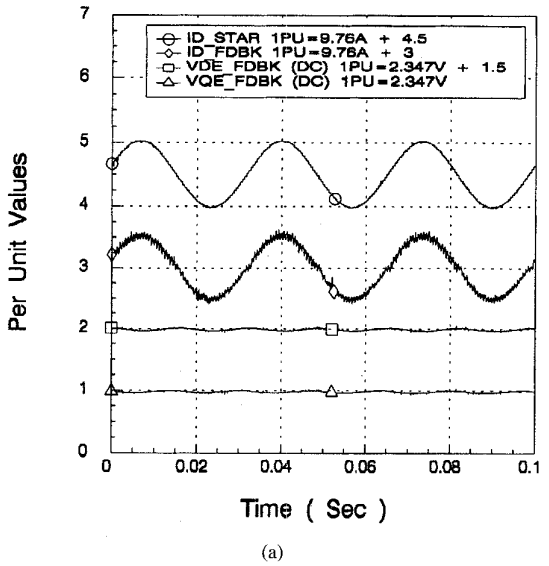


(a)

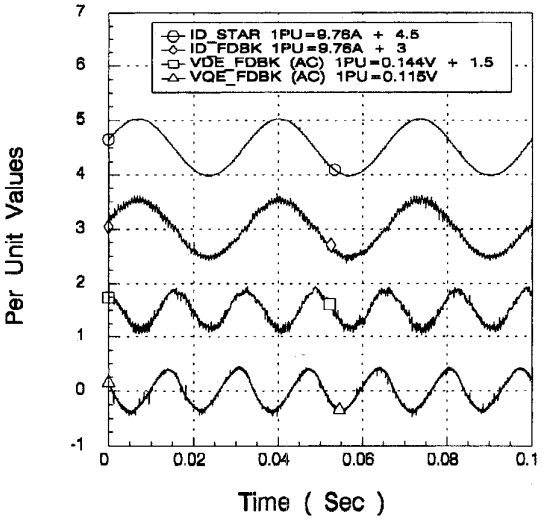


(b)

Fig. 11. (a) Single-phase excitation: dc-coupled feedback. (b) Single-phase excitation: ac-coupled feedback.

within the measurement. Through synchronous sampling, the second harmonic is easily filtered. A simple form of this synchronous sampler is given by (12). $V_x$ is the signal to be filtered, $T_\mu$ the processor update rate of the sampling module, $F_e$ the single-phase excitation frequency, and $N\text{count}$ the number of samples in one cycle of the excitation frequency

$$V_{x\,\text{ave}} = T_\mu F_e \sum_{i=1}^{N\,\text{count}} V_x. \tag{12}$$

Tests were performed on the 20-hp machine of Fig. 4. Fig. 12 shows the transient inductance obtained by the frequency-based procedure as a function of excitation frequency at various current levels. The value of transient inductance obtained from the transient test is also plotted. As the excitation frequency increases, the single-phase excitation method yields values approaching that of the transient method.

TABLE I
COMMISSIONING RESULTS

| HP | Poles | Motor Voltage | $L_\sigma$ Tuned | $L_\sigma$ Single Phase | $L_\sigma$ Transient | Torque Linearity Error * |
|---|---|---|---|---|---|---|
| 7.5 | 4 | 460 | | 15.717 mH | | - 1.30 % |
| 7.5 | 10 | 460 | 10.199 mH | 10.199 mH | 10.99 mH | approx 0 |
| 20 | 4 | 460 | 6.974 mH | 6.974 mH | 4.31 mH | approx 0 |
| 20 | 4 | 460 | 7.047 mH | 7.59 mH | 4.821 mH | 0.80 % |
| 200 | 4 | 460 | 683 uH | 683 uH | 516 uH | - 2.34 % |
| 500 | 4 | 460 | 314 uH | 298.5 uH | 257 uH | - 5.80 % |
| 1250 | 6 | 575 | | 189 uH | | 0.32 % |

*Torque Linearity Error was based on single-phase established $L_\sigma$ values.

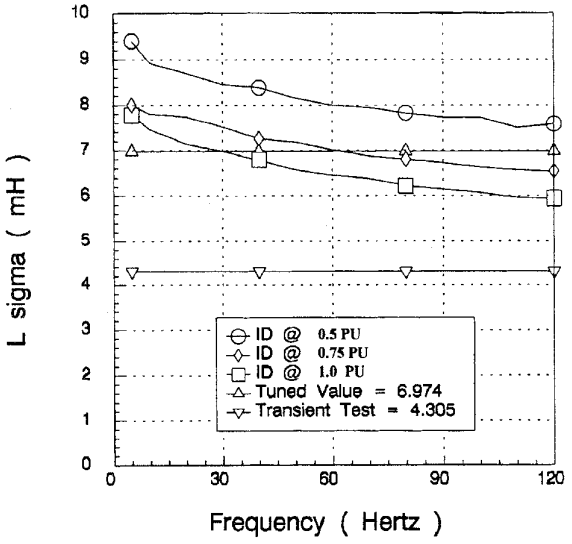


Fig. 12. Experimental results for frequency-based determination of $L_\sigma$ as a function of current.

Furthermore, the results indicate the value of the transient inductance depends on the amplitude of the single-phase current. By making a sequence of tests at specified current levels, the self-commissioning procedure can estimate the variation in the transient inductance with load.

The transient performance of a IFOC depends on the degree of decoupling between the rotor's $q$ and $d$ axes. One method of measuring the quality of FO is to observe the machine's terminal voltage in the synchronous frame following a step change in the commanded torque [2]. Tests were performed on a 4-pole, 460-V, 200-hp induction machine to evaluate the relative quality of FO resulting from a MRAC with reference parameter values obtained by the two deterministic commissioning procedures. The motor was controlled in a torque mode at 900 r/min. Just before the reference change, the FOC's adaptation was disabled; thus, the most recent estimate of the slip gain was employed based on the reference model's transient inductance. The results for a step change from no-load to 1 p.u. are shown in Fig. 13.

Fig. 13(a) shows the transient response for the case when the MRAC employs the transient inductance obtained from the transient test. The degree of FO is observed by the response of the $q$-$d$ axes voltages; the greater the oscillation the more coupled the rotor circuits. Note the substantial oscillation at slip frequency present in the voltages and the level change in both components, clearly indicating a degradation in FO. The torque exhibits a similar oscillation.

Fig. 13(b) shows the response to the same transient, but with the MRAC employing the reference transient inductance obtained from the single-phase steady-state commissioning procedure. The contrast in performance with the results of Fig. 13(a) is striking. Fig. 13(b) shows significantly improved dynamic response; a small oscillation exists with no level shift in the $q$-axis voltage indicating excellent transient and steady-state FO.

Field commissioning tests were performed on numerous laboratory machines. The dynamometer-tuned inductance and inductances obtained from the frequency based and transient commissioning procedures are presented in Table I. The variation in the transient inductance obtained from the frequency-based commissioning procedure follows the expected trend with increasing horsepower. The values obtained from the transient procedure are consistently lower, again suggesting a skin-effect influence. Using the single-phase frequency-based transient inductance, the MRAC establishes a slip gain $(K_s)$ that produces excellent torque linearity. The substantially larger error observed with the 500-hp data is a consequence of a 460-V motor operating on a 575-V drive; thus, demonstrating the effects of inadequate voltage feedback resolution.

The frequency-based single-phase self-commissioning procedure also provides an estimate of the rotor resistance. Experimental evaluation of the procedure was conducted on a 5-hp wound rotor induction motor. This motor configuration provides an accurate evaluation of the rotor resistance estimation. The results of the tests are shown in Fig. 14. The commissioning procedure was repeated for the range of rotor resistances indicated along the abscissa with the estimated value plotted along the ordinate. All resistance measurements are referred to the stator. Three plots are shown: the measured sum of the stator and rotor resistances, the estimated value of the sum at one-half of rated motor current, and the estimated

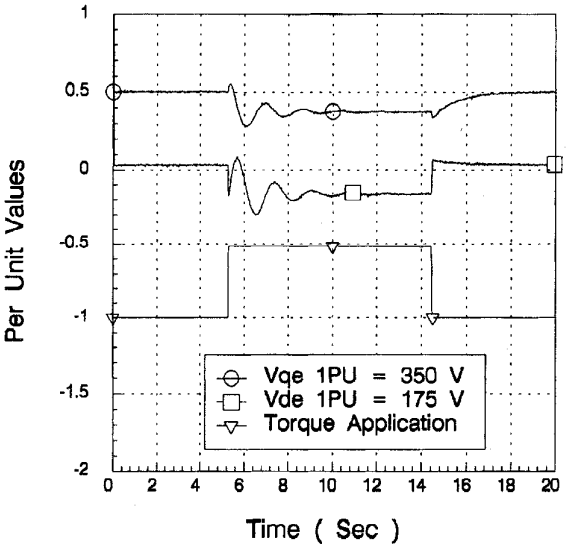


(a)

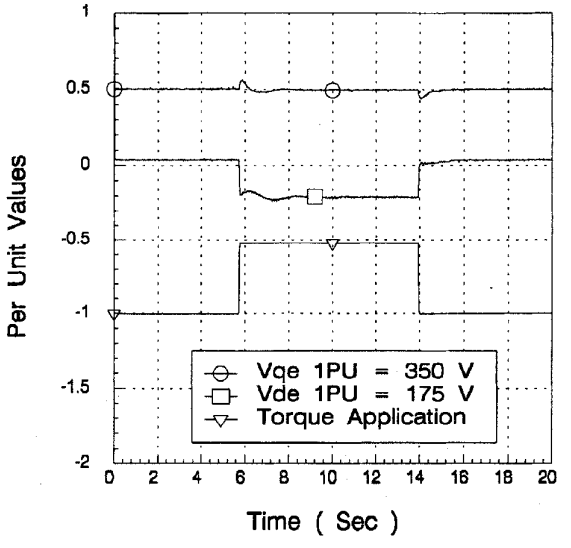


(b)

Fig. 13. Experimental results: (a) Transient response with $L_\sigma$ from transient test. (b) Transient response with $L_\sigma$ from single-phase test.

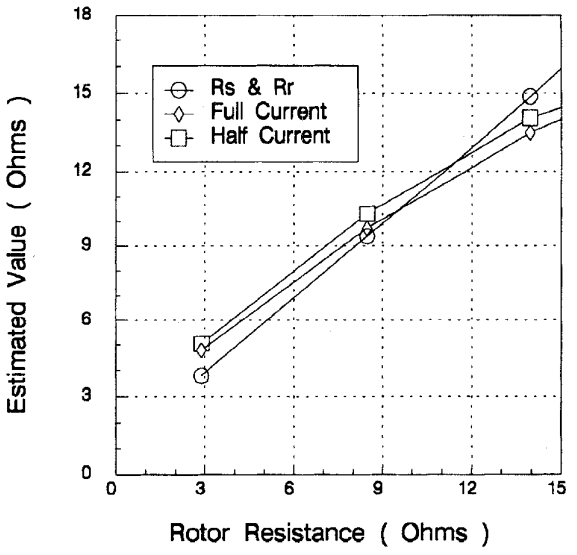


Fig. 14. Rotor resistance estimation.

TABLE II
5-HP INDUCTION MACHINE

| | | |
|---|---|---|
| 460 volts | $r_s = 2.2380\ \Omega$ | $L_s = 0.3115$ H |
| 4 pole | $r_r = 0.8556\ \Omega$ | $L_r = 0.3115$ H |
| 1775 rpm | $H = 0.0158$ kg-m$^2$ | $L_m = 0.2971$ H |

TABLE III
10-HP INDUCTION MACHINE

| | | |
|---|---|---|
| 460 volts | $r_s = 0.476\ \Omega$ | $L_s = 0.125$ H |
| 4 pole | $r_r = 1.600\ \Omega$ | $L_r = 0.124$ H |
| 1775 rpm | $H = 0.0286$ kg-m$^2$ | $L_m = 0.121$ H |

value of the sum at rated motor current. The excitation frequency was 30 Hz. The estimated sum of the stator and rotor resistance is in very good agreement with the measured values.

The results show the single-phase frequency-based procedure capable of providing an initial value for the rotor resistance. The rotor resistance estimate together with the results from the flux commissioning procedure provides an initial value for the slip gain of the IFOC.

## V. CONCLUSION

The paper examines field commissioning procedures for establishing the transient inductance and rotor resistance of an induction machine. The paper presents two deterministic techniques for parameter estimation: the transient and frequency domain approaches. The paper demonstrates the difficulties with the transient method. Experimental results show the transient inductance obtained from the transient technique significantly underestimates the fundamental component value. The deterioration in FO resulting from employing the transient method's value within the reference model of a MRAC is demonstrated through analytical and experimental results.

The paper proposes a single-phase current excitation method compatible with established hardware platforms. The frequency-based procedure, which excites the machine with single-phase sinusoidal current, was analyzed and experimentally evaluated. The results showed this technique is capable of accurately estimating the transient inductance and rotor resistance, provided the excitation frequency is

constrained to reduce skin effect. Furthermore, the dependency of the transient inductance on current or load level and the field commissioning procedure's ability to identify it were demonstrated.

## APPENDIX

The machine parameters for the 5- and 10-hp induction motors employed in the simulation results are given in Tables II and III, respectively.

## REFERENCES


[1] L. C. Zai and T. A. Lipo, "An extended kalman filter approach to rotor time constant measurement in PWM induction motor drives," in *Conf. Rec. of the IEEE IAS Annual Meeting*, 1987, pp. 177–183.

[2] T. M. Rowan, R. J. Kerkman, and D. Leggate, "A simple on-line adaption for indirect field orientation of an induction machine," *IEEE Trans. Ind. Applicat.*, vol. 27, no. 4, pp. 720–727, July/Aug. 1991.

[3] H. Schierling, "Self-commissioning—A novel feature of modern inverter-fed induction motor drives," in *IEE Conf. Power Electron., Variable Speed Drives*, London, U.K., July 13–15, 1988, pp. 287–290.

[4] R. Joetten and H. Schierling, "Adaptive and self-commissioning control for a drive with induction motor and voltage source inverter," in *2nd European Conf. Power Electron., Applicat.*, Grenoble, France, Sept. 22–24, 1987, pp. 489–492.

[5] M. Ruff and H. Grotstollen, "Identification of the saturated mutual inductance of an asynchronous motor at standstill by recursive least squares algorithm," in *5th European Conf. Power Electron., Applicat.*, Brighton, U.K., 1993, vol. 5, pp. 103–108.

[6] M. Depenbrock and N. R. Klaes, "Determination of the induction machine parameters and their dependencies on saturation," in *Conf. Rec. IEEE IAS Annu. Meeting*, pt. 1, 1989.

[7] N. R. Klaes, "Accurate off-line identification of the operating point dependent induction machine parameters," presented at the EDS '90—Electrical Drives Symp., Capri, Italy, Sept. 25–27, 1990.

[8] G. Heinemann and W. Leonhard, "Self-tuning field oriented control of an induction motor drive," in *Proc. 1990 Int. Power Electron. Conf. (IPEC)*, Tokyo, Japan, Apr. 2–6, 1990, pp. 465–472.

[9] C. Wang, D. W. Novotny, and T. A. Lipo, "An automated rotor time constant measurement for indirect field-oriented drives," *IEEE Trans. Ind. Applicat.*, vol. IA-24, no. 1, pp. 151–159, Jan./Feb. 1988.

[10] P. C. Krause, "Method of multiple reference frames applied to the analysis of symmetrical induction machinery," *IEEE Trans. Power Apparatus and Systems*, vol. 87, pp. 218–227, Jan. 1968.


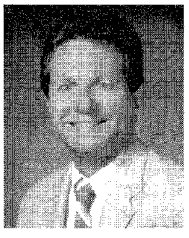

**Russel J. Kerkman** (S'67–M'76–SM'88) received the B.S.E.E., M.S.E.E., and Ph.D. degrees in electrical engineering from Purdue University, West Lafayette, IN, in 1971, 1973, and 1976, respectively.

From 1976 to 1980, he was an Electrical Engineer in the Power Electronics Laboratory of Corporate Research and Development, General Electric Company, Schenectady, NY. He is currently a Senior Principal Engineer for the Allen Bradley Company, Mequon, WI. His current interests include the modeling and control of general purpose industrial drives, adaptive control applied field oriented induction machines, and the application of observers to ac machines.

**Jerry D. Thunes** (S'77–M'77) received the B.S.E.E.T. degree from the Milwaukee School of Engineering, Milwaukee, WI, in 1977 and the M.S.E.E degree from Marquette University, Milwaukee, in 1985.

He has been employed at the Allen Bradley Company, Mequon, WI, since 1977, where he is currently a Project Engineer. His current interests are ac motor control and power device technology.

Mr. Thunes is a Registered Professional Engineer in the State of Wisconsin.

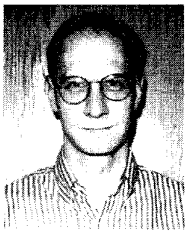

**Timothy M. Rowan** (M'87) received the B.S.E.E. degree from Marquette University, Milwaukee, WI, in 1980, and the M.S.E.E. and Ph.D. degrees from the University of Wisconsin, Madison, in 1982, and 1985, respectively.

He has been employed at the Allen Bradley Company, Mequon, WI, since 1983, where he is currently a Principal Engineer. His current interests are in the development and analysis of ac drives.

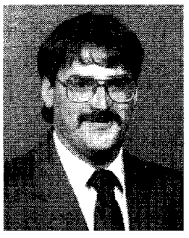

**David W. Schlegel** (S'89) received the A.A.S. degree in electrical power engineering technology from the Milwaukee School of Engineering, Milwaukee, WI, in 1990. He will complete the requirements of the B.S.E.E.T. degree from the Milwaukee School of Engineering, Milwaukee, WI, in May 1996.

He has been employed at the Allen Bradley Company, Mequon, WI, since 1979, where he is currently a Senior Development Technician.